JOURNAL OF VIROLOGY, Apr. 1996, p. 2230–2236 Vol. 70, No. 4
0022-538X/96/$04.00+0

*ts*1-Induced Spongiform Encephalomyelopathy: Physical Forms of High-Mobility DNA in Spinal Cord Tissues of Paralyzed Mice Are Products of Premature Termination of Reverse Transcription

PAUL F. SZUREK AND BENJAMIN RIX BROOKS*

Neurology and Research Services, William S. Middleton Memorial Veterans Medical Center, and Departments of Neurology and Medical Microbiology-Immunology, University of Wisconsin—Madison Medical School, Madison, Wisconsin 53705-2286

Received 12 July 1995/Accepted 18 December 1995

***ts*1 is a temperature-sensitive mutant of Moloney murine leukemia virus that causes hind-limb paralysis in mice. In tissues of the central nervous systems of paralyzed moribund FVB/N mice, a major component of the unintegrated viral DNA of *ts*1 consists of highly mobile physical forms of viral-specific DNA (HM DNA). Previous studies with ecotropic virus-specific polarity probes showed that the gp70-coding region of the *env* gene in the HM DNA was minus-sense single-stranded DNA. The physical forms of the HM DNA have now been characterized in more detail with additional ecotropic virus-specific probes that hybridized to the p15E-coding region of the *env* gene and two locations within the U3 region of the long terminal repeat. Two major classes of HM DNA were found: class I molecules consist of short minus-sense single-stranded DNA; class II molecules are partial DNA duplexes that are longer than the class I molecules. The two classes of HM DNA molecules are intermediate products of reverse transcription of the viral RNA of *ts*1. Since tissues that are infected with cytopathic retroviruses may contain high levels of unintegrated viral DNA, the HM DNA may have a role in inducing neurodegeneration in the central nervous systems of mice that are infected with *ts*1.**

*ts*1 is one of a number of temperature-sensitive mutants of Moloney murine leukemia virus (MoMuLV) that cause neurodegenerative disease in mice (31–33). It was recently shown that the spinal cord tissues of paralyzed moribund FVB/N mice that were infected with *ts*1 contained, as a major component of the total unintegrated physical forms of virus-specific DNA, elevated levels of minus-sense single-stranded high-mobility (HM) DNA. This DNA was identified by probes that hybridized to the gp70-coding region of the *env* gene (30). These initial studies suggested that the physical forms of HM DNA may be premature termination products of reverse transcription of viral RNA. In dividing fibroblasts in vitro, reverse transcription is rapid, and only low amounts of intermediate products of reverse transcription are detectable. However, in quiescent cells, the rate of reverse transcription is much slower (6, 28), and there is accumulation of premature termination products of reverse transcription (9, 39, 47, 48). The central nervous systems (CNS) of paralyzed moribund mice that are infected with *ts*1 provide an ideal system for studying early intermediate steps of retroviral replication in vivo, since there is a high density of quiescent cells in the CNS. The accumulation of these physical forms of unintegrated HM DNA has previously been correlated with the development of clinical signs of *ts*1-induced neurodegenerative disease (30). Our results indicate that the HM DNA that is present in the spinal cord tissue in vivo is synthesized by a mechanism that is consistent with current models for reverse transcription by retroviruses (2, 12, 14, 15, 23, 42).

While there is a general model for the mechanism of reverse transcription, the complete mechanism of reverse transcription is not entirely understood (19, 42). Virions of MoMuLV contain two copies of the viral plus-sense RNA genome. During reverse transcription, strand transfer reactions may be either intrastrand (14) or interstrand (12, 15). Studies using spleen necrosis virus-based retroviral vectors have shown that both intrastrand and interstrand transfer reactions occur in tissue culture cells (12, 14). However, the physical forms of single-stranded DNA that are generated during reverse transcription depend on whether intermediate proviral DNA forms are drawn as circular (2, 15, 42) or linear (12, 14, 23). Both of the proposed circular and linear intermediates yield the same proviral double-stranded DNA product.

Reverse transcription of the plus-sense viral RNA template begins at the $tRNA^{Pro}$ primer binding site (PBS), and it proceeds to the 5′ end of the RNA genome to form minus-strong-stop DNA. The plus-sense viral RNA template between the 5′ end of the viral RNA and the PBS is then digested by RNase H. The RNase H digestion exposes the newly synthesized single-stranded cDNA copy of the small terminal repeat at the 3′ end (3′ R region) of the minus-strong-stop DNA. Complete synthesis of the 3′ R region is not necessary for strand transfer to occur (23). The 3′ R region of the minus-strong-stop DNA then forms base pairs to the complementary r region at the 3′ end (3′ r region) of the plus-sense viral RNA template. The base-pairing reaction between the minus-sense 3′ R region and the plus-sense 3′ r region that forms the R-r hybrid is the first strand transfer reaction. In intrastrand transfers, the 3′ R region of the minus-strong-stop DNA is transferred to the 3′ r region of the original viral RNA template, whereas in interstrand transfers, the 3′ R region of the minus-strong-stop DNA is transferred to the 3′ r region of the second viral RNA template.

Reverse transcription of the viral RNA template continues by extending the minus-strong-stop DNA. After extension of the minus-strong-stop DNA proceeds beyond the polypurine tract (PPT), RNase H nicks the viral RNA at the PPT primer site (25). Reverse transcriptase then synthesizes plus-strong-stop DNA from the PPT primer site to the 5′ end of the PBS by using the viral minus-sense DNA as a template. The remainder of the plus-strong-stop DNA is synthesized by using 18 nucleotides (nt) of the $tRNA^{Pro}$ as a template, and reverse

* Corresponding author. Phone: (608) 262-7090. Fax: (608) 263-0412. Electronic mail address: brooks@neurology.wisc.edu.

transcription terminates at the first methylated nucleoside (^{m1}A) of tRNA^{Pro}. Reverse transcriptase-associated RNase H then digests the tRNA^{Pro} template. After a second strand transfer reaction, reverse transcription is completed by strand displacement synthesis (42).

In this study, we characterized the physical forms of the HM DNA that are present in the spinal cord tissues of mice with *ts*1-induced spongiform encephalomyelopathy by Southern blot hybridization with additional ecotropic virus-specific probes that hybridized to the p15E-coding region of the *env* gene and to two locations in the U3 region of the long terminal repeat (LTR). In addition to the high levels of minus-sense single-stranded DNA that were reported previously (30), these experiments indicated that the HM DNA in the spinal cord tissues of paralyzed moribund mice contains high levels of partial DNA duplexes and low levels of free plus-sense single-stranded DNA. These elevated levels of intermediate products of reverse transcription provide strong evidence that an important pathogenetic feature of the neurodegenerative disease induced by *ts*1 in susceptible mice may be significant infection of quiescent cells of the CNS in vivo.

MATERIALS AND METHODS

Viruses. A molecular clone of *ts*1, *ts*1-92b, was propagated in TB cells as described previously (30).

Vectors containing inserts of viral DNA. Plasmids p1 (46), p22 (46), and penv-SB and recombinant M13 clones (+) M13-env-SB and (−) M13-env-BS [(+) and (−) indicate plus sense and minus sense, respectively] have been described previously (30). Plasmid p15E-SE was constructed by inserting the 122-bp (nt 7487 to 7608) *Spe*I-*Eco*RV fragment of plasmid p22 into the *Xba*I and *Eco*RV sites of pSP72 (Promega, Madison, Wis.). Plasmid pU3-NP was constructed by inserting the 57-bp (nt 7879 to 7937) *Nla*III-*Pvu*II fragment of p22 into the *Bbu*I (*Sph*I) and *Pvu*II sites of pSP73. In the *Nla*III-*Pvu*II fragment of *ts*1, there are two single deletions in base, nt 7930 and 7931, relative to that of MoMuLV (43). Plasmid pU3-SS was constructed by blunt ending the 55-bp (nt 8095 to 8149) *Sin*I fragment of p22 with T4 DNA polymerase and then inserting it into the *Sma*I site of pSP73.

(+) M13-U3-SS18 and (−) M13-U3-SS19 were constructed by inserting the *Xba*I-*Sac*I fragment of pU3-SS into M13mp18 and M13mp19, respectively. The inserted fragments of the recombinant M13 clones contained some sequences of the polylinker of pSP73. The polarity of the inserted fragments of the M13mp18 recombinant clones was plus sense, whereas that of the inserted fragments of M13mp19 was minus sense. The polarity of the insert of each of the recombinant M13 clones was verified by nucleotide sequencing (31, 33). The single-stranded phagemid clone, (+) ss22TZ6, was constructed by inserting the *Hin*dIII-*Eco*RI fragment of p22 into phagemid pTZ18R (18) as described previously (29). Nucleotides were numbered by the method of Shinnick et al. (26).

Inoculation and monitoring of mice. FVB/N mice (Taconic, Germantown, N.Y.) (34) were inoculated intraperitoneally with 10^5 to 10^6 infectious units of virus in 0.05 ml of growth medium within 24 h of birth (30). Mice were monitored for clinical signs of paralysis by being suspended by their tails (30).

Purification of total cellular DNA. Total cellular DNA was purified from the spinal cord tissue of paralyzed moribund mice as described previously (30).

Probes for ecotropic virus-specific DNA sequences. Restriction fragments were purified by electroelution from an agarose gel. The eluted double-stranded DNA restriction fragments were radiolabeled with [α-^{32}P]dCTP with a Prime-a-Gene kit (Promega) as described previously (30). The ecotropic virus-specific env-SB probe is the radiolabeled 302-bp *Sma*I-*Bam*HI restriction fragment of penv-SB, and it hybridizes to the gp70-coding region of the *env* gene of *ts*1 (30). The 122-bp *Spe*I-*Eco*RV p15E-SE probe hybridizes to the p15E-coding region of the *env* gene of *ts*1, but it does not hybridize to sequences in the total cellular liver DNA of an uninfected FVB/N mouse (mouse 80). The hybridization site of the p15E-SE probe is similar to that of the 154-bp (nt 7506 to 7659) ecotropic virus-specific *Hae*III fragment of AKV virus that was described by Herr et al. (10). The 57-bp *Nla*III-*Pvu*II U3-NP probe is contained within an *Nla*III-*Sau*96I fragment of MoMuLV (68 bp, nt 7879 to 7946) that was shown to be ecotropic virus specific for the U3 region of the LTR by Simard et al. (27). The 55-bp *Sin*I U3-SS probe is contained within a *Sau*96I fragment of MoMuLV (55 bp, nt 8095 to 8149) that was shown to be ecotropic virus specific for the U3 region of the LTR by Huang et al. (13). Probes U3-NP and U3-SS do not hybridize to sequences in the total cellular liver DNA of an uninfected FVB/N mouse (mouse 80).

Polarity probes for the recombinant (+) M13mp18 and (−) M13mp19 clones were radiolabeled by the method of primer extension as described previously (30). The radiolabeled polarity probes that were complementary to the plus-sense inserts of M13mp18 recombinant clones were minus sense, and the polarity probes that were complementary to the minus-sense inserts of M13mp19 recombinant clones were plus sense.

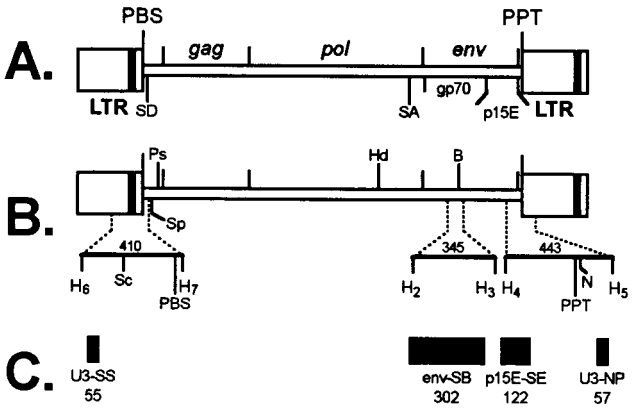

FIG. 1. Locations of the ecotropic-specific probes in the proviral DNA of *ts*1 that hybridize to specific *Hae*III fragments. (A) Genetic map of the viral DNA of *ts*1. The LTR region is not drawn to scale. SD, splice donor; SA, splice acceptor. (B) Locations of the *Hae*III fragments that hybridize to the ecotropic virus-specific probes. The lengths of the *Hae*III fragments are in base pairs. (C) Locations of the ecotropic virus-specific probes. The lengths of the probes are in base pairs. Probe U3-SS is a 55-bp (nt 8095 to 8149) *Sin*I fragment that hybridizes to a 410-bp (nt 8069 to 8264 and 1 to 214) H_6-H_7 *Hae*III fragment. Probe env-SB is a 302-bp (nt 6236 to 6537) *Sma*I-*Bam*HI fragment that hybridizes to a 345-bp (nt 6239 to 6583) H_2-H_3 *Hae*III fragment. Probe p15E-SE is a 122-bp (nt 7487 to 7608) *Spe*I-*Eco*RV fragment that hybridizes to a 443-bp (nt 7506 to 7948) H_4-H_5 *Hae*III fragment. Probe U3-NP is a 57-bp (nt 7879 to 7937) *Nla*III-*Pvu*II fragment that hybridizes to the same 443-bp H_4-H_5 *Hae*III fragment as does probe p15E-SE. Restriction sites: B, *Bam*HI; Hd, *Hin*dIII; H, *Hae*III; N, *Nhe*I; Ps, *Pst*I; Sc, *Sac*I; Sp, *Spe*I.

Digestion of total cellular DNA with S1 nuclease. Total cellular DNA was digested with S1 nuclease in a volume of 100 μl under conditions that were described previously (30).

Southern blot hybridization. The method for Southern blot hybridization was described previously (30).

RESULTS

Mapping the HM DNA with ecotropic virus-specific probes. We have previously shown that a major component of the unintegrated *ts*1-specific DNA present in the spinal cord tissues of paralyzed moribund mice consists of minus-sense single-stranded HM DNA. The minus-sense single-stranded HM DNA was detected in the total cellular spinal cord DNA of paralyzed moribund mice by Southern blot hybridization with a plus-sense polarity probe, (+) M13-env-BS, that contained sequences of the gp70-coding region of the *env* gene (Fig. 1) (30). To further determine the composition of the HM DNA, we mapped the HM DNA with three additional ecotropic virus-specific probes, p15E-SE, U3-NP, and U3-SS. The location of the hybridization site in the genome of *ts*1 for each of the probes is shown in Fig. 1.

Within 24 h of birth, FVB/N mice were inoculated with *ts*1. Mice were sacrificed (n = 77) when they were both paralyzed and moribund as described previously (30) between 27 and 55 days postinfection (median, 35 days postinfection). Forty-four mice (57%) had tonic spasms of the arms and legs when they were twirled by the tail (45). The total cellular DNA of the spinal cords of the sacrificed mice was pooled. Ecotropic virus-specific sequences in the undigested total cellular spinal cord DNA were detected by Southern blot hybridization with four double-stranded ecotropic virus-specific probes, env-SB, p15E-SE, U3-NP, and U3-SS (Fig. 2). Each of the probes hybridized to HM DNA in the lower portions of lanes 1 to 4 (Fig. 2).

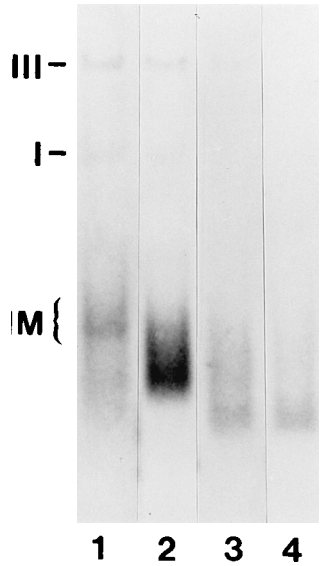

FIG. 2. Mapping the HM DNA with double-stranded ecotropic virus-specific probes. The total cellular DNA from the spinal cords of 77 paralyzed moribund mice that were infected with *ts*1 was pooled. Untreated DNA samples of 29 μg each were fractionated by 0.8% agarose gel electrophoresis and transferred to a Nytran Plus membrane. Ecotropic virus-specific sequences were detected by Southern blot hybridization with probes env-SB (lane 1), p15E-SE (lane 2), U3-NP (lane 3), and U3-SS (lane 4).

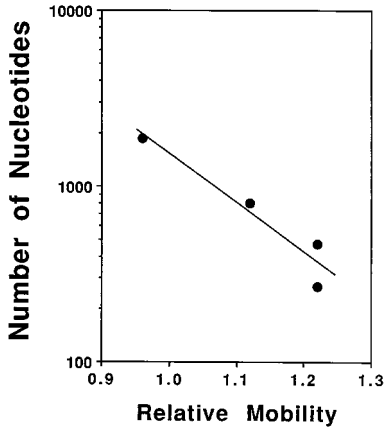

FIG. 3. Relative mobilities of HM DNA molecules that hybridize to the double-stranded ecotropic virus-specific probes. The number of nucleotides between the 3′ end of the hybridization site for each of the probes (log scale) is plotted versus the relative mobility of the leading edge of the band of HM DNA in Fig. 2. The mobilities are relative to that of bromophenol blue.

There was weak hybridization to the relatively less abundant unintegrated physical forms I (supercoil) and III (linear) for probes env-SB (lane 1) and p15E-SE (lane 2). These bands were much stronger in a longer exposure of the autoradiograph (data not shown). Hybridization to physical forms I and III was not detectable for the shortest probes, U3-NP (lane 3) and U3-SS (lane 4). These results were consistent with previous results that showed that the HM DNA was the most abundant physical form of unintegrated viral DNA in the spinal cord tissues of paralyzed moribund mice (30). The relative intensity of the band of HM DNA for each of the probes does not necessarily correlate to the relative abundance of sequences that hybridized to each of the probes since the probes had different lengths, different percentages of G+C content, and different amounts of the C base (Table 1).

The relative mobility of the leading edge of the band of HM DNA decreased as the distance (in nucleotides) of the 3′ end of the hybridization site in the HM DNA increased from the PBS (Fig. 3). This result indicated that the probes were hybridizing to HM DNA molecules that had a minimum length that was equal to the distance between the hybridization site and the PBS, as previously proposed by Szurek and Brooks (30). Therefore, HM DNA synthesis was most likely initiated at the PBS as predicted by current models of retroviral reverse transcription (2, 12, 14, 15, 23, 42). Since HM molecules that hybridized to the env-SB and p15E-SE probes were longer than the distance between the PPT site and the PBS, it was possible that plus-sense DNA synthesis had been initiated at the PPT primer site.

TABLE 1. Base compositions of the double-stranded DNA probes

Probe	Length (bp)	% A+T	% G+C
env-SB	302	48	52
p15E-SE	122	56	44
U3-NP	57	63	37
U3-SS	55	49	51

Most long HM DNA molecules contained a region of double-stranded DNA. To determine if most long HM DNA molecules were partial DNA duplexes, a Southern blot of undigested total cellular DNA was hybridized to the (−) M13-env-SB and (+) M13-env-BS polarity probes (Fig. 4). (+) M13-env-BS hybridized to the undigested HM DNA (Fig. 4, lane 4), whereas (−) M13-env-SB did not hybridize to the undigested HM DNA (lane 1). To confirm our previous results that (+) M13-env-BS was hybridizing to single-stranded HM DNA, the total cellular DNA of the spinal cord was digested with *Hae*III, which digests both single-stranded DNA and double-stranded DNA (11, 30). The (−) M13-env-SB and (+) M13-env-BS

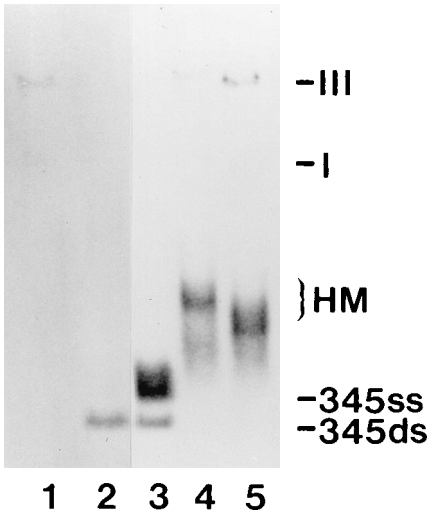

FIG. 4. Most long HM DNA molecules contained a region of double-stranded DNA. Total cellular DNA (29 μg) was either undigested or digested with restriction endonucleases. Ecotropic virus-specific sequences in the DNAs were detected by Southern blot hybridization at 68°C with [α-^{32}P]dCTP-labeled probes (−) M13-env-SB (lanes 1 and 2) and (+) M13-env-BS (lanes 3 to 5). Lanes: 1, undigested; 2, *Hae*III digested; 3, *Hae*III digested; 4, undigested; 5, *Nhe*I digested. The positions of the 345-nt single-stranded DNA (ss) and 345-nt double-stranded DNA (ds) markers are indicated.

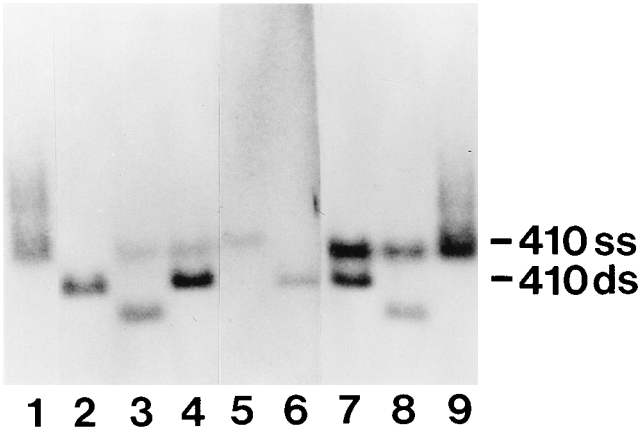

FIG. 5. Determining the polarity of the HM DNA in the U3 region of the LTR with (−) M13-U3-SS18 and (+) M13-U3-SS19. Total cellular DNA (29 μg) was either undigested or digested with nucleases. Ecotropic virus-specific sequences in the DNAs were detected by Southern blot hybridization at 68°C with [α-^{32}P]dCTP-labeled probes (−) M13-U3-SS18 (lanes 1 to 4), U3-SS (lanes 5, 6), and (+) M13-U3-SS19 (lanes 7 to 9). Lanes: 1, undigested; 2, digested with *Hae*III followed by S1 nuclease; 3, doubly digested with *Hae*III and *Sac*I; 4, *Hae*III digested; 7, *Hae*III digested; 8, doubly digested with *Hae*III and *Sac*I; 9, undigested. Lanes that contained 410-nt markers: 5, 860 ng of (+) ss22TZ6 single-stranded DNA (ss) digested with *Hae*III; 6, 520 ng of plasmid p22 digested with *Hae*III. ds, double-stranded DNA.

probes hybridize to a 345-nt H_2-H_3 *Hae*III fragment in the genome of *ts*1 (Fig. 1). Both probes hybridized to the lower double-stranded H_2-H_3 *Hae*III fragment (lanes 2 and 3), but only the (+) M13-env-BS probe hybridized to the upper single-stranded H_2-H_3 *Hae*III fragment (lane 3). If the HM DNA was pure single-stranded DNA, it should have been resistant to digestion by restriction enzymes that were specific for double-stranded DNA. However, when the total cellular DNA was digested with *Nhe*I, there was a decrease in the mobility of all of the detectable hybridizing HM DNA molecules (lane 5). There is only one *Nhe*I site in the genome of MoMuLV (26) which is also present in the genome of *ts*1 (43). Since the *Nhe*I site is located 31 nt downstream from the PPT site (Fig. 1), most long HM DNA molecules contained duplex DNA at the 3′ end.

HM DNA hybridized to both plus-sense and minus-sense polarity probes in the U3 region of the LTR. To confirm that the population of HM DNA molecules contained both plus-sense and minus-sense DNA, the HM DNA was further analyzed with polarity probes that were specific for the U3 region of the genome of *ts*1. Polarity probes (−) M13-U3-SS18 and (+) M13-U3-SS19 hybridize to a 410-nt H_6-H_7 *Hae*III fragment in the U3 region of the LTR in the genome of *ts*1 (Fig. 1). Both (−) M13-U3-SS18 and (+) M13-U3-SS19 hybridized to undigested HM DNA (Fig. 5, lanes 1 and 9, respectively). This result showed that the HM DNA contained both plus-sense and minus-sense DNA in the U3 region of the LTR.

To determine if (−) M13-U3-SS18 and (+) M13-U3-SS19 were hybridizing to single-stranded HM DNA, the total DNA was digested with *Hae*III. Both probes hybridized to two *Hae*III bands (Fig. 5, lanes 4 and 7). The lower bands had mobilities that were approximately the same as that of the 410-bp double-stranded DNA marker (lane 6). Since both of the lower bands were digested by *Sac*I (lanes 3 and 8), they were segments of double-stranded DNA that contained sequences of the H_6-H_7 *Hae*III fragment (Fig. 1). Both of the upper bands (Fig. 5, lanes 4 and 7) had a mobility that was approximately the same as that of the 410-nt single-stranded DNA marker. Moreover, the upper bands were resistant to *Sac*I (lanes 3 and 8), which indicated that they were segments of single-stranded DNA. The upper band in lane 4 was sensitive to S1 nuclease (lane 2), which confirmed that the HM DNA contained free plus-sense single-stranded DNA. Therefore, in the U3 region of the LTR, the HM DNA contained physical forms of both free plus-sense single-stranded DNA and free minus-sense single-stranded DNA. Additional experiments indicated that some of the plus-sense HM DNA was base paired to a complementary strand of minus-sense single-stranded HM DNA in the form of a DNA duplex.

The 3′ end of the HM DNA was double stranded. It has been shown that digestion with *Nhe*I decreases the mobility of long HM molecules (Fig. 4, lane 5). This result indicated that the 3′ end of long HM molecules was double-stranded DNA. To characterize this putative double-stranded region of HM DNA, the physical forms of the HM DNA were analyzed with the (+) M13-U3-SS19 probe, which hybridizes to the 3′ end of the genome of *ts*1. When (+) M13-U3-SS19 was hybridized to undigested total cellular DNA, the HM DNA was heterogeneous in size (Fig. 6, lane 4). However, when the total cellular DNA was digested with S1 nuclease, the heterogeneous band disappeared, and the hybridizing product was a fragment (lane 5) that had a mobility that was approximately the same as that of the 0.7-kb marker (lane 9). Therefore, it may be concluded that the HM DNA contained a region of double-stranded DNA.

To show that the duplex region of the HM DNA was covalently attached to long molecules of HM DNA but was not covalently attached to short HM DNA molecules, the total cellular DNA was digested with *Nhe*I. The heterogeneous band of HM DNA disappeared, and the product was a wide band of hybridizing DNA (Fig. 6, lane 6). Since it has already been shown that HM DNA contained regions of both single-stranded DNA and double-stranded DNA, it was possible that the wide band in lane 6 contained both of these physical forms. When the total cellular DNA was doubly digested with *Nhe*I and S1 nuclease, the wide band in lane 6 disappeared, and the product was an S1 nuclease-resistant fragment (lane 7) that

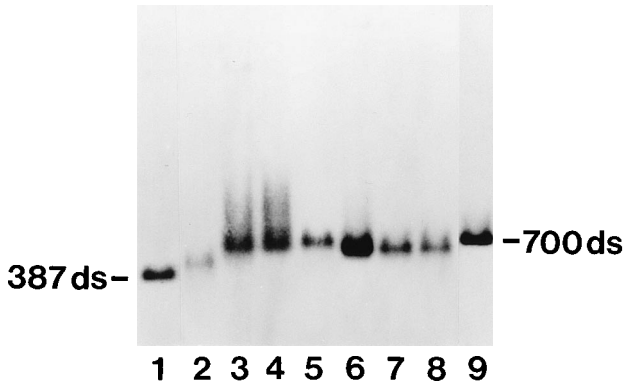

FIG. 6. Analysis of the duplex region of HM DNA with S1 nuclease and restriction endonucleases. Total cellular DNA (29 μg) was either undigested or digested with nucleases. Ecotropic virus-specific sequences in the DNAs were detected by Southern blot hybridization at 68°C with [α-^{32}P]dCTP-labeled probes U3-SS (lanes 1 and 9) and (+) M13-U3-SS19 (lanes 2 to 8). Lanes: 2, digested with *Sac*I followed by S1 nuclease; 3, *Sac*I digested; 4, undigested; 5, S1 nuclease digested; 6, *Nhe*I digested; 7, digested with *Nhe*I followed by S1 nuclease; 8, doubly digested with *Nhe*I and *Spe*I and then with S1 nuclease. Lanes that contained markers: 1, 600 ng of plasmid p22 doubly digested with *Nhe*I and *Sac*I; 9, 600 ng of plasmid p22 doubly digested with *Nhe*I and *Spe*I. The positions of both the 387- and 700-bp double-stranded DNA (ds) markers are indicated.

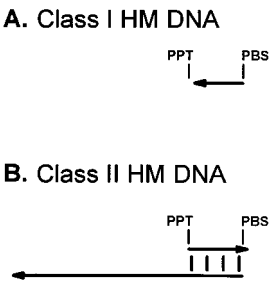

FIG. 7. Models for the physical forms of HM DNA. (A) Class I HM DNA; (B) class II HM DNA. Arrows denote strands of DNA that are of variable length. Viral RNA and $tRNA^{Pro}$ templates are not shown.

had a mobility that was less than that of the fragment in lane 5. *Nhe*I had cleaved the fragment in lane 5 to yield the hybridizing product in lane 7, whereas S1 nuclease digested the short minus-sense molecules of HM DNA. If the long HM DNA molecules had been pure minus-sense single-stranded DNA, they would have hybridized to the probe in lane 6, and lane 6 would have appeared the same as the control lane (lane 4).

To confirm that duplex DNA was covalently attached to minus-sense single-stranded HM DNA, the total cellular DNA was digested with *Sac*I. The *Sac*I digest yielded a result that was much different from that of the *Nhe*I digest because the hybridization site of (+) M13-U3-SS19 was located downstream from the *Nhe*I site but upstream from the *Sac*I site (Fig. 1). Differences between the mobilities of the *Sac*I-digested HM DNA (Fig. 6, lane 3) and the undigested control HM DNA (lane 4) were not detectable. However, *Sac*I did digest the HM DNA since the total cellular DNA that was doubly digested with both *Sac*I and S1 nuclease yielded a small fragment of hybridizing double-stranded DNA as a digestion product (lane 2). S1 nuclease released the small hybridizing fragment in lane 2 from the *Sac*I-digested HM DNA (lane 3) by digesting minus-sense single-stranded HM DNA. Therefore, the small hybridizing fragment in lane 2 was covalently linked to the minus-sense single-stranded HM DNA in lane 3. Since S1 nuclease-digested DNA contained only one large S1 nuclease-resistant fragment (lane 5), the small hybridizing fragment in lane 2 was a *Sac*I digestion product of the large S1 nuclease-resistant fragment in lane 5. Therefore, the large S1 nuclease-resistant fragment in lane 5 was covalently linked to the minus-sense single-stranded HM DNA. Therefore, it can be concluded that most long molecules of HM DNA contained double-stranded DNA at the 3′ end and that most short HM molecules consisted of free minus-sense single-stranded HM DNA.

The double digest of HM DNA with *Nhe*I and *Spe*I in lane 8 of Fig. 6 yielded an S1 nuclease-resistant fragment that had the same mobility as the S1 nuclease-resistant *Nhe*I digestion product in lane 7, but it had a mobility that was less than that of the *Nhe*I-*Spe*I marker in lane 9. This result showed that the duplex region of the HM DNA did not extend beyond the 3′ end of the PBS as shown in the restriction map (Fig. 1).

DISCUSSION

The major component of unintegrated *ts*1-specific DNA in cells of the CNS of paralyzed moribund mice consists of HM DNA (30). HM DNA in the spinal cord tissues of paralyzed moribund mice is composed of a heterogeneous population of incomplete reverse transcription products of viral RNA. There are two major classes of physical forms of HM DNA (Fig. 7). Class I HM DNA molecules (Fig. 7A) are pure minus-sense single-stranded DNA molecules that are initiated at the PBS but terminate before the PPT primer site, and they have a size that is less than the length of one LTR (26). Possibly, some of these class I HM DNA molecules were synthesized in mature virus particles prior to infection (37, 49). Class II HM DNA molecules (Fig. 7B) are double stranded between the PPT primer site and the PBS, and they are single stranded upstream of the PPT primer site. This finding in vivo is similar to the earlier results in vitro of DesGroseillers et al. (7), who showed that plus-strand synthesis in MuLVs begins before completion of synthesis of 8.2-kb minus-strand DNA.

The PPT site was used as the sole primer for synthesizing the plus-sense strand of the DNA duplex. Alternate multiple plus-strand initiation sites at nt 7219, 7221, and 7237 in the N-terminal coding region of p15E have been identified in vitro (24). If these alternate priming sites were used in vivo in the CNS, there should have been three fragments that had a *Sac*I site (nt 8233) at the 3′ end in lane 2 of Fig. 6) with lengths of 1,015 bp (nt 7219 to 8233), 1,013 bp (nt 7221 to 8233), and 997 bp (nt 7237 to 8233). However, the fragment in lane 2 had an electrophoretic mobility that was slightly slower than that of the 387-bp (nt 7847 to 8233) *Nhe*I-*Sac*I marker in lane 1. Most likely the fragment in lane 2 was the 5′ end of plus-strong-stop DNA (PPT-*Sac*I) which would have a length of 418 bp (nt 7816 to 8233), as predicted from the sequence of MoMuLV (26). Therefore these alternate priming sites do not appear to be used in the spinal cord tissues of mice that are infected with *ts*1.

Free plus-sense single-stranded DNA was also detected in the HM DNA with the (−) M13-U3-SS18 probe (Fig. 6, lane 4). Free plus-sense single-stranded DNA has not been previously detected in MoMuLV-infected cells. In some current schematic diagrams of the product of the second strand transfer reaction (12, 15), the 3′ end of free plus-sense DNA has been drawn such that the PBS region is base paired to the PBS region at the 3′ end of full-length 8.2-kb minus-strand DNA. Presumably, this intermediate product of reverse transcription is formed by the plus-sense strand of plus-strong-stop DNA jumping from the 5′ end of 8.2-kb minus-strand DNA to the 3′ end of 8.2-kb minus-strand DNA. It is not known whether this intermediate is actually formed during reverse transcription. Some retroviruses generate free plus-sense viral DNA by a different mechanism. In avian retroviruses, such as Rous sarcoma virus, physical forms of free plus-sense subgenomic regions of viral DNA are generated at multiple initiation sites (35). Some MuLVs also generate plus-sense DNA at multiple initiation sites, but free plus-sense DNA forms have not been isolated. In endogenous reactions in vitro with a B-tropic strain of MuLV, B-C-11, DesGroseillers et al. (7) have shown that plus-strand synthesis is initiated at multiple start sites at both ends of the genome. This segmented mechanism of proviral DNA synthesis has not been demonstrated for MoMuLV. In tissues of the CNS of paralyzed moribund mice, the origin of the low amount of U3-specific free plus-sense single-stranded DNA is currently not known.

In paralyzed moribund mice, high levels of class II HM DNA accumulated in the spinal cord tissue by 35 days postinfection. Previously we reported that low levels of HM DNA appeared as early as 10 days postinfection (30). Therefore, the class II HM DNA had at least 25 days to accumulate in the infected neural cells. Over this long period of time, it is not known why the class II molecules accumulated instead of undergoing the second strand-transfer reaction. Bowerman et al. (3) have shown that retroviral RNA is reverse transcribed in a virion-derived porous nucleoprotein complex in the cytoplasm of infected cells. The nucleocapsid protein of MoMuLV is required for the strand transfer reaction (2). Possibly, the viral

nucleoprotein complexes that contained the class II HM DNA degraded as they aged in the cytoplasm of quiescent neural cells. The putative degraded viral nucleoprotein complexes might have been unsuitable for the second strand transfer reaction, and therefore class II HM DNA molecules accumulated in the quiescent neural cells.

Inefficient reverse transcription of viral RNA in quiescent neural cells might also have been responsible for the synthesis of the incomplete proviral forms of HM DNA (9, 39, 48). The upper H_2-H_3 *Hae*III band of single-stranded DNA in the gp70-coding region of the *env* gene (Fig. 4, lane 3) was heterogeneous in size compared with the upper H_6-H_7 *Hae*III band of single-stranded DNA in the U3 region of the LTR (Fig. 5, lane 7). Previously we proposed that the heterogeneity of this band of DNA was due to single-strand conformational polymorphisms (20) that were generated by an error-prone reverse transcriptase (38). However, if this were the case, the major location of genetic variation in HM DNA would be different from that in viral genomes that are synthesized in productively infected cells since the greatest sequence variation in retroviruses is in the U3 region of the LTR (5).

Another possibility for the heterogeneity of the upper H_2-H_3 *Hae*III band of single-stranded DNA in the gp70-coding region of *env* (Fig. 4, lane 3) is that the error rate of the reverse transcriptase was enhanced by low deoxynucleoside triphosphate (dNTP) pools in quiescent neural cells. Martinez et al. (17) have found that low dNTP pools induce hypermutagenesis by the reverse transcriptase of human immunodeficiency virus type 1. Furthermore, Goulaouic et al. (9) have found that only the early steps of reverse transcription take place in dNTP-depleted serum-starved tissue culture cells that are infected with MoMuLV. The heterogeneity in size of the upper H_2-H_3 *Hae*III fragment could also be due to premature termination at a pause site (1) to yield a heterogeneous population of *Hae*III fragments that had sizes that were less than the full length of the H_2-H_3 fragment, or alternatively, pausing could induce strand transfer-mediated mutagenesis (44). It is also possible that over the course of the 35-day incubation period, there was some degradation of the single-stranded region of the class II HM DNA by a cell-coded exonuclease. For human immunodeficiency virus type 1, Zack et al. (47) have shown that partially reverse transcribed viral DNA is labile and rapidly degraded in quiescent T cells, whereas Spina et al. (28) have identified stable complete reverse transcription products in quiescent CD4 lymphocytes in vitro. In neural cells that are infected with *ts*1 in vivo, it is not known if there is degradation of HM DNA over time, but the sharpness of the S1 nuclease-resistant band in Fig. 6 (lane 5) indicated that the 3′ end of class II HM molecules was stable.

The role of the physical forms of HM DNA in inducing neurodegenerative disease in mice that are infected with *ts*1 is not known. However, it is possible than the DNA duplex region of the class II HM DNA molecules has a role in elevating gene expression in infected cells. Weng et al. (41) have shown that the LTR of MoMuLV *trans* activates AP-1-inducible genes. The level of the mRNA of the c-*jun* proto-oncogene is increased over 60-fold. Major histocompatibility complex class I antigen expression is also increased by *trans* activation. Yoshioka et al. (45) have shown that transgenic mice that express elevated levels of the major histocompatibility complex class I antigen in oligodendrocytes develop neurodegenerative disease with some features of the oligodendroglial pathogenesis that is seen in mice that are infected with *ts*1. Normal cellular functions of neural cells may be sensitive to abnormal levels of cellular gene expression. Transgenic mice that overexpress the interleukin-6 gene (4) and the *Mos* proto-oncogene (22) also develop neurodegenerative disease. Previously we proposed that *ts*1 abortively superinfects quiescent cells in the CNS (30). It is possible that multiple copies of class II HM molecules in these putative abortively superinfected neural cells lead to abnormal levels of gene expression, which in turn leads to neurodegenerative disease. Unintegrated retroviral DNA has been correlated with cytotoxicity for a number of retroviruses (8, 21, 36, 40). Possibly the retroviral DNA itself is not cytotoxic, but the products induced by *trans* activation may be cytotoxic. Experiments have not yet been performed to show that the class II HM DNA does elevate gene expression in the CNS by *trans* activation. It is also possible that the HM DNA does not have a role in inducing neurodegenerative disease, but the high levels of HM DNA in the CNS of paralyzed moribund mice indicate that abortive infection of quiescent neural cells may be an important feature of the pathogenesis of *ts*1-induced spongiform encephalomyelopathy that requires further study.

ACKNOWLEDGMENTS

This work was supported in part by a Department of Veterans Affairs (DVA) Merit Review grant (B.R.B.), Research and Development funds from the University of Wisconsin Department of Neurology, and shared equipment was provided by a DVA Geriatrics Research Educational and Clinical Center grant.

REFERENCES

1. **Abbotts, J., K. Bebenek, T. A. Kunkel, and S. H. Wilson.** 1993. Mechanism of HIV-1 reverse transcriptase. J. Biol. Chem. **268:**10312–10323.
2. **Allain, B., M. Lapadat-Tapolsky, C. Berlioz, and J. L. Darlix.** 1994. Transactivation of the minus-strand DNA transfer by nucleocapsid protein during reverse transcription of the retroviral genome. EMBO J. **13:**973–981.
3. **Bowerman, B., P. O. Brown, J. M. Bishop, and H. E. Varmus.** 1989. A nucleoprotein complex mediates the integration of retroviral DNA. Genes Dev. **3:**469–478.
4. **Campbell, I. L., C. R. Abraham, E. Masliah, P. Kemper, J. D. Inglis, M. B. A. Oldstone, and L. Mucke.** 1993. Neurologic disease induced in transgenic mice by cerebral overexpression of interleukin 6. Proc. Natl. Acad. Sci. USA **90:**10061–10065.
5. **Coffin, J. M.** 1986. Genetic variation in AIDS viruses. Cell **46:**1–4.
6. **Collin, M., and S. Gordon.** 1994. The kinetics of human immunodeficiency virus reverse transcription are slower in primary human macrophages than in a lymphoid cell line. Virology **200:**114–120.
7. **DesGroseillers, L., E. Rassart, M. Zollinger, and P. Jolicoeur.** 1982. Synthesis of murine leukemia viral DNA in vitro: evidence for plus-strand DNA synthesis at both ends of the genome. J. Virol. **42:**326–330.
8. **Donahue, P. R., S. L. Quackenbush, M. V. Gallo, C. M. C. DeNoronha, J. Overbaugh, E. A. Hoover, and J. I. Mullins.** 1991. Viral genetic determinants of T-cell killing and immunodeficiency disease induction by the feline leukemia virus FeLV-FAIDS. J. Virol. **65:**4461–4469.
9. **Goulaouic, H., F. Subra, J. F. Mouscadet, S. Carteau, and C. Auclair.** 1994. Exogenous nucleosides promote the completion of MoMuLV DNA synthesis in G0-arrested Balb c/3T3 fibroblasts. Virology **200:**87–97.
10. **Herr, W., D. Schwartz, and W. Gilbert.** 1983. Isolation and mapping of cDNA hybridization probes specific for ecotropic and nonecotropic murine leukemia proviruses. Virology **125:**139–154.
11. **Horiuchi, K., and N. D. Zinder.** 1975. Site-specific cleavage of single-stranded DNA by a *Hemophilus* restriction endonuclease. Proc. Natl. Acad. Sci. USA **72:**2555–2558.
12. **Hu, W., and H. M. Temin.** 1990. Retroviral recombination and reverse transcription. Science **250:**1227–1233.
13. **Huang, M., C. Simard, D. G. Kay, and P. Jolicoeur.** 1991. The majority of cells infected with the defective murine AIDS virus belong to the B-cell lineage. J. Virol. **65:**6562–6571.
14. **Jones, J. S., R. W. Allan, and H. M. Temin.** 1994. One retroviral RNA is sufficient for synthesis of viral DNA. J. Virol. **68:**207–216.
15. **Lauermann, V., and J. D. Boeke.** 1994. The primer tRNA sequence is not inherited during Ty1 retrotransposition. Proc. Natl. Acad. Sci. USA **91:**9847–9851.
16. **Maniatis, T., A. Jeffrey, and H. van deSande.** 1975. Chain length determination of small double- and single-stranded DNA molecules by polyacrylamide gel electrophoresis. Biochemistry **14:**3787–3794.
17. **Martinez, M. A., J. P. Vartanian, and S. Wain-Hobson.** 1994. Hypermutagenesis of RNA using human immunodeficiency virus type 1 reverse transcriptase and biased dNTP concentrations. Proc. Natl. Acad. Sci. USA **91:**11787–11791.

18. **Mead, D. A., E. Szczesna-Skorupa, and B. Kemper.** 1986. Single-stranded DNA 'blue' T7 promoter plasmids: a versatile tandem promoter system for cloning and protein engineering. Protein Eng. **1:**67–74.
19. **Miller, M. D., B. Wang, and F. D. Bushman.** 1995. Human immunodeficiency virus type I preintegration complexes containing discontinuous plus strands are competent to integrate in vitro. J. Virol. **69:**3938–3944.
20. **Orita, M., H. Iwahana, H. Kanazawa, K. Hayashi, and T. Sekiya.** 1989. Detection of polymorphisms of human DNA by gel electrophoresis as single-strand conformation polymorphisms. Proc. Natl. Acad. Sci. USA **86:**2766–2770.
21. **Pang, S., Y. Koyanagi, S. Miles, C. Wiley, H. V. Vinters, and I. S. Y. Chen.** 1990. High levels of unintegrated HIV-1 DNA in brain tissue of AIDS dementia patients. Nature (London) **343:**85–89.
22. **Propst, F., M. P. Rosenberg, L. C. Cork, R. M. Kovatch, S. Rauch, H. Westphal, J. Khillan, N. T. Schulz, G. F. Vande Woude, and P. E. Newmann.** 1990. Neuropathological changes in transgenic mice carrying copies of a transcriptionally activated *Mos* protooncogene. Proc. Natl. Acad. Sci. USA **87:**9703–9708.
23. **Ramsey, C. A., and A. T. Panganiban.** 1993. Replication of the retroviral terminal repeat sequence during in vivo reverse transcription. J. Virol. **67:** 4114–4121.
24. **Rattray, A. J., and J. J. Champoux.** 1987. The role of Moloney murine leukemia virus RNase H activity in the formation of plus-strand primers. J. Virol. **61:**2843–2851.
25. **Rattray, A. J., and J. J. Champoux.** 1989. Plus-strand priming by Moloney murine leukemia virus. J. Mol. Biol. **208:**445–456.
26. **Shinnick, T. M., R. A. Lerner, and J. G. Sutcliffe.** 1981. Nucleotide sequence of Moloney murine leukaemia virus. Nature (London) **293:**543–548.
27. **Simard, C., M. Huang, and P. Jolicoeur.** 1994. Murine AIDS is initiated in the lymph nodes draining the site of inoculation, and the infected B cells influence T cells located at distance, in noninfected organs. J. Virol. **68:**1903–1912.
28. **Spina, C. A., J. C. Guatelli, and D. D. Richman.** 1995. Establishment of a stable, inducible form of human immunodeficiency virus type 1 DNA in quiescent CD4 lymphocytes in vitro. J. Virol. **69:**2977–2988.
29. **Szurek, P. F.** 1990. Ph.D. thesis. The University of Texas, Houston.
30. **Szurek, P. F., and B. R. Brooks.** 1995. Development of physical forms of unintegrated retroviral DNA in mouse spinal cord tissue during *ts*1-induced spongiform encephalomyelopathy: elevated levels of a novel single-stranded form in paralyzed mice. J. Virol. **69:**348–356.
31. **Szurek, P. F., E. Floyd, P. H. Yuen, and P. K. Y. Wong.** 1990. Site-directed mutagenesis of the codon for Ile-25 in gPr80^{env} alters the neurovirulence of *ts*1, a mutant of Moloney murine leukemia virus TB. J. Virol. **64:**5241–5249.
32. **Szurek, P. F., P. H. Yuen, J. K. Ball, and P. K. Y. Wong.** 1990. A Val-25-to-Ile substitution in the envelope precursor polyprotein, gPr80^{env}, is responsible for the temperature sensitivity, inefficient processing of gPr80^{env}, and neurovirulence of *ts*1, a mutant of Moloney murine leukemia virus TB. J. Virol. **64:**467–475.
33. **Szurek, P. F., P. H. Yuen, R. Jerzy, and P. K. Y. Wong.** 1988. Identification of point mutations in the envelope gene of Moloney murine leukemia virus TB temperature-sensitive paralytogenic mutant *ts*1: molecular determinants for neurovirulence. J. Virol. **62:**357–360.
34. **Taketo, M., A. C. Schroeder, L. E. Mobraaten, K. B. Gunning, G. Hanten, R. R. Fox, T. H. Roderick, C. L. Stewart, F. Lilly, C. T. Hansen, and P. A. Overbeek.** 1991. FVB/N: an inbred mouse strain preferable for transgenic analyses. Proc. Natl. Acad. Sci. USA **88:**2065–2069.
35. **Taylor, J. M., A. Cywinski, and J. K. Smith.** 1983. Discontinuities in the DNA synthesized by an avian retrovirus. J. Virol. **48:**654–659.
36. **Temin, H. M.** 1988. Mechanisms of cell killing/cytopathic effects by nonhuman retroviruses. Rev. Infect. Dis. **10:**399–405.
37. **Trono, D.** 1992. Partial reverse transcripts in virions from human immunodeficiency and murine leukemia viruses. J. Virol. **66:**4893–4900.
38. **Varela-Echavarria, A., N. Garvey, B. D. Preston, and J. P. Dougherty.** 1992. Comparison of Moloney murine leukemia virus mutation rate with the fidelity of its reverse transcriptase *in vitro*. J. Biol. Chem. **267:**24681–24688.
39. **Varmus, H. E., T. Padgett, S. Heasley, G. Simon, and J. M. Bishop.** 1977. Cellular functions are required for the synthesis and integration of avian sarcoma virus-specific DNA. Cell **11:**307–319.
40. **Weller, S. K., A. E. Joy, and H. M. Temin.** 1980. Correlation between cell killing and massive second-round superinfection by members of some subgroups of avian leukosis virus. J. Virol. **33:**494–506.
41. **Weng, H., S. Y. Choi, and D. V. Faller.** 1995. The Moloney leukemia retroviral long terminal repeat *trans*-activates AP-1 inducible genes and AP-1 transcription factor binding. J. Biol. Chem. **270:**13637–13644.
42. **Whiting, S. H., and J. J. Champoux.** 1994. Strand displacement synthesis capability of Moloney murine leukemia virus reverse transcriptase. J. Virol. **68:**4747–4758.
43. **Wong, P. K. Y., P. F. Szurek, E. Floyd, K. Saha, and B. R. Brooks.** 1991. Alteration from T- to B-cell tropism reduces thymic atrophy and cytocidal effects in thymocytes but not neurovirulence induced by *ts*1, a mutant of Moloney murine leukemia virus TB. Proc. Natl. Acad. Sci. USA **88:**8991–8995.
44. **Wu, W., B. M. Blumberg, P. J. Fay, and R. A. Bambara.** 1995. Strand transfer mediated by human immunodeficiency virus reverse transcriptase *in vitro* is promoted by pausing and results in misincorporation. J. Biol. Chem. **270:** 325–332.
45. **Yoshioka, T., L. Feigenbaum, and G. Jay.** 1991. Transgenic mouse model for central nervous system demyelination. Mol. Cell. Biol. **11:**5479–5486.
46. **Yuen, P. H., D. Malehorn, C. Knupp, and P. K. Y. Wong.** 1985. A 1.6-kilobase-pair fragment in the genome of the *ts*1 mutant of Moloney murine leukemia virus TB that is associated with temperature sensitivity, nonprocessing of Pr80^{env}, and paralytogenesis. J. Virol. **54:**364–373.
47. **Zack, J. A., S. J. Arrigo, S. R. Weitsman, A. S. Go, A. Haislip, and I. S. Y. Chen.** 1990. HIV-1 entry into quiescent primary lymphocytes: molecular analysis reveals a labile, latent viral structure. Cell **61:**213–222.
48. **Zack, J. A., A. M. Haislip, P. Krogstad, and I. S. Y. Chen.** 1992. Incompletely reverse-transcribed human immunodeficiency virus type 1 genomes in quiescent cells can function as intermediates in the retroviral life cycle. J. Virol. **66:**1717–1725.
49. **Zhu, J., and J. M. Cunningham.** 1993. Minus-strand DNA is present within murine type C ecotropic retroviruses prior to infection. J. Virol. **67:**2385–2388.